


## ARTICLE



# Astrocytes modulate extracellular neurotransmitter levels and excitatory neurotransmission in dorsolateral striatum via dopamine D2 receptor signaling

Louise Adermark<sup>1,2</sup> , Oona Lagström<sup>1</sup>, Anna Loftén<sup>1,3</sup>, Valentina Licheri<sup>1</sup>, Amy Havenäng<sup>1</sup>, Eleonora Anna Loi<sup>1</sup>, Rosita Stomberg<sup>1</sup>, Bo Söderpalm<sup>1,3</sup>, Ana Domi<sup>1</sup> and Mia Ericson<sup>1</sup>

© The Author(s), under exclusive licence to American College of Neuropsychopharmacology 2021

Astrocytes provide structural and metabolic support of neuronal tissue, but may also be involved in shaping synaptic output. To further define the role of striatal astrocytes in modulating neurotransmission we performed *in vivo* microdialysis and *ex vivo* slice electrophysiology combined with metabolic, chemogenetic, and pharmacological approaches. Microdialysis recordings revealed that intrastriatal perfusion of the metabolic uncoupler fluorocitrate (FC) produced a robust increase in extracellular glutamate levels, with a parallel and progressive decline in glutamine. In addition, FC significantly increased the microdialysate concentrations of dopamine and taurine, but did not modulate the extracellular levels of glycine or serine. Despite the increase in glutamate levels, *ex vivo* electrophysiology demonstrated a reduced excitability of striatal neurons in response to FC. The decrease in evoked potentials was accompanied by an increased paired pulse ratio, and a reduced frequency of spontaneous excitatory postsynaptic currents, suggesting that FC depresses striatal output by reducing the probability of transmitter release. The effect by FC was mimicked by chemogenetic inhibition of astrocytes using G<sub>i</sub>-coupled designer receptors exclusively activated by designer drugs (DREADDs) targeting GFAP, and by the glial glutamate transporter inhibitor TFB-TBOA. Both FC- and TFB-TBOA-mediated synaptic depression were inhibited in brain slices pre-treated with the dopamine D2 receptor antagonist sulpiride, but insensitive to agents acting on presynaptic glutamatergic autoreceptors, NMDA receptors, gap junction coupling, cannabinoid 1 receptors,  $\mu$ -opioid receptors, P2 receptors or GABA<sub>A</sub> receptors. In conclusion, our data collectively support a role for astrocytes in modulating striatal neurotransmission and suggest that reduced transmission after astrocytic inhibition involves dopamine.

*Neuropsychopharmacology* (2022) 47:1493–1502; <https://doi.org/10.1038/s41386-021-01232-x>

## INTRODUCTION

The quiescent astrocyte has long been acknowledged for its structural and metabolic support of neurotransmission. However, research performed during the last few decades suggests that astrocytes also are involved in signal processing, and may integrate neurotransmission in a complex manner [1, 2]. In fact, astrocytes appear to constitute an integral element of the neuronal synapse, and one single astrocyte can interact with hundreds of neuronal dendrites, thereby functioning as an active processing bridge for synaptic interaction and crosstalk [2–5]. Astrocytes can also modulate neuronal signaling in a long-lasting manner by promoting and inhibiting the removal of specific synaptic connections, and by regulating synaptic plasticity mechanisms [6–9]. Importantly, even though receptors for more or less all neurotransmitters are expressed by astrocytes, they have been shown to specifically respond to activation of discrete axon pathways, and may also be able to discriminate between specific neuronal circuits [10, 11]. The tight structural and functional interaction between astrocytes and neurons may thus be vital for normal brain functioning [12, 13].

Astrocytes present a large range of modulatory activities that potentiate or depress the release of several neurotransmitters. Especially astrocytes have been recognized as important regulators of glutamatergic neurotransmission. Glial glutamate-transporters GLAST/EAAT1 and GLT-1/EAAT2 clear glutamate from the extra-synaptic space, and the transport is driven by the ion gradients of K<sup>+</sup> and Na<sup>+</sup> [14, 15]. Following astrocytic uptake, glutamate is degraded into the non-excitatory amino acid glutamine, which is released back to the extracellular space where it is taken up by neurons [7, 16, 17]. Changes in astrocytic glutamate clearance, and/or astrocytic glutamate transporters, have been considered to be core features in several neurological disorders [12, 13, 18–20], and mice with a genetic deletion of GLAST exhibit phenotypic abnormalities, including cognitive and executive dysfunction [21, 22]. Astrocytes can further modulate excitatory neurotransmission and NMDA receptor activation by regulating the abundance of the co-agonist glycine via glycine transporter 1 and 2 [14, 23]. Lastly, astrocytes may release gliotransmitters such as glutamate, ATP/adenosine, D-serine, taurine, and homocysteic acid, which further modulate excitatory neurotransmission [24–27].

<sup>1</sup>Addiction Biology Unit, Department of Psychiatry and Neurochemistry, Institute of Neuroscience and Physiology, The Sahlgrenska Academy, University of Gothenburg, Gothenburg, Sweden. <sup>2</sup>Department of Pharmacology, Institute of Neuroscience and Physiology, The Sahlgrenska Academy, University of Gothenburg, Gothenburg, Sweden. <sup>3</sup>Beroendekliniken, Sahlgrenska University Hospital, Gothenburg, Sweden. ✉email: [louise.adermark@gu.se](mailto:louise.adermark@gu.se)

Received: 10 July 2021 Revised: 28 October 2021 Accepted: 30 October 2021  
Published online: 22 November 2021

The striatum is the major input nucleus to the basal ganglia. Striatal pathology has primarily been associated with movement disorders, but psychiatric morbidity has also been linked to abnormalities in the basal ganglia and their allied nuclei [28–30]. The dorsolateral part of the striatum (DLS) is recruited during action learning, consolidation of motor skills, and habitual performances [31–33], and has also been linked to drug-seeking behavior and drug addiction [34–36]. We have previously shown that striatal astrocytes are extensively interconnected and form a syncytium that allows wide-spread communication [37, 38]. Later research has also implicated striatal astrocytes in synaptic communication and plasticity [9, 39], supporting a key role for astrocytes in modulating striatal neurotransmission.

The aim of this study was to further investigate by which mechanisms astrocytes control the extracellular environment and shape synaptic activity. Since neurons and astrocytes express an overlapping array of receptors and ion channels, single pharmacological manipulation is not sufficient to disentangle the role of astrocytes in modulating synaptic activity. One compound that has been used to inhibit astrocytes is the metabolic uncoupler fluorocitrate (FC). Fluorocitrate gradually and reversibly decreases metabolic activity by blocking aconitase, an enzyme utilized in the tricarboxylic acid (TCA) cycle [40]. The specificity for astrocytes over neurons has been shown by monitoring a decline in glutamine formation from [<sup>14</sup>C]acetate, a substrate that enters the glial cells selectively, while not showing effects on the metabolism of [<sup>14</sup>C]glucose, which enters neurons [41–43]. Fluorocitrate decreases ATP levels [44], and impairs astrocyte function, including calcium signaling and potassium uptake [45, 46]. Mice with metabolically inhibited astrocytes furthermore show deficits in motor-skill learning, a behavior that involves recruitment of the DLS [33, 46, 47]. In the present study, using a battery of metabolic, chemogenetic and pharmacological approaches, we suppressed astrocytic activity, and monitored changes in neurotransmission using *in vivo* microdialysis and *ex vivo* electrophysiology in the dorsolateral striatum of male Wistar rats.

## MATERIALS AND METHODS

### Experimental outline

The overall aim of this study was to assess the role of astrocytes in modulating striatal neurotransmission. One approach to inhibit astrocytes was through metabolic inhibition using the compound fluorocitrate (FC). Effects on neurotransmission by FC were monitored by *in vivo* microdialysis ( $n = 12$  rats), and *ex vivo* electrophysiology ( $n = 66$  rats). Astrocyte function was also inhibited using G<sub>i</sub>-coupled designer receptors exclusively activated by designer drugs (DREADDs) targeting GFAP in DLS (*ex vivo* electrophysiology,  $n = 18$  rats; immunohistochemistry,  $n = 4$  rats), and by the glial glutamate transporter inhibitor TFB-TBOA (*ex vivo* electrophysiology,  $n = 7$  rats).

### Animals

Male Wistar rats (Envigo, The Netherlands) were group housed with a 12 h dark/light cycle and ad libitum access to water and food. Rats were allowed to adapt to the novel environmental conditions (room temperature of 20 °C, relative humidity 65%, and a regular light–dark cycle with lights on at 07:00 AM and off at 07:00 PM) for at least one week prior to any procedure. The experiments were approved by the Ethics Committee for Animal Experiments, Gothenburg, Sweden.

### Drugs

The metabolic uncoupler DL-Fluorocitric acid barium salt (FC) was dissolved in either Ringer's solution (microdialysis) containing (in mM): 140 NaCl, 1.2 CaCl<sub>2</sub>, 3.0 KCl and 1.0 MgCl<sub>2</sub>, or artificial cerebrospinal fluid (aCSF) (electrophysiology), containing (in mM): 124 NaCl, 4.5 KCl, 2 CaCl<sub>2</sub>, 1 MgCl<sub>2</sub>, 26 NaHCO<sub>3</sub>, 1.2 NaH<sub>2</sub>PO<sub>4</sub>, and 10 D-glucose, to a final concentration of 50 μM (microdialysis) or 5 μM (electrophysiology). These concentrations were based on previous *in vivo* and *in vitro* studies showing impaired

lactate and glucose oxidation, and estimating an equilibration of 15% of FC across the dialysis membrane [48–50]. The DREADDs agonist Clozapine N-oxide dihydrochloride (CNO) was dissolved in dimethyl-sulfoxide (DMSO) to 20 mM, and further diluted to 10 or 2 μM in aCSF. For pharmacological regulation of glutamatergic neurotransmission, the NMDA receptor antagonist DL-2-Amino-5-phosphonopentanoic acid (APV), was dissolved in H<sub>2</sub>O (MilliQ) to 25 mM and used at 50 μM, the AMPA receptor antagonist 6-cyano-7-nitroquinoxaline-2,3-dione (CNQX) disodium salt hydrate was dissolved in H<sub>2</sub>O to 20 mM and further diluted to 10 μM, the mGluR2/3 antagonist LY 341495 disodium salt was dissolved in H<sub>2</sub>O to 1 mM and used at 200 nM, while the glutamate-transporter inhibitor TFB-TBOA was dissolved in DMSO to 10 mM and further diluted in aCSF to 200 nM. Glutamine (1 mM) was dissolved in aCSF shortly before use. The GABA<sub>A</sub> antagonist (-)-bicuculline methiodide was dissolved in H<sub>2</sub>O to 20 mM and used at 20 μM, while the cannabinoid 1 receptor antagonist AM251 was dissolved in DMSO to 20 mM and diluted in aCSF to 2 μM. The gap junction inhibitor carbenoxolone disodium was dissolved in H<sub>2</sub>O (100 mM) and diluted in aCSF to a final concentration of 100 μM, while the P2 receptor antagonist pyridoxal phosphate-6-azo(benzene-2,4-disulfonic acid) tetrasodium salt hydrate (PPADs) was dissolved in H<sub>2</sub>O to 10 mM and used at 30 μM. The μ-receptor antagonist CTAP was dissolved in H<sub>2</sub>O to 0.5 mM and used at 50 nM. Dopamine D1 receptors were blocked using R(+)-SCH-23390 hydrochloride, dissolved in H<sub>2</sub>O 20 mM and used at 0.5 μM, while dopamine D2 receptors were blocked with (±)-sulpiride, dissolved in EtOH to 20 mM and further diluted to 5 μM in aCSF. Drugs were purchased from Sigma Aldrich (Stockholm, Sweden), or Tocris (Bristol, UK).

### Surgery for viral injections and microdialysis

Animals (weighing 170–190 g for viral injections and 270–340 g for microdialysis) were anesthetized with 4% isoflurane (Forene, Baxter, Kista, Sweden) and placed in a stereotaxic frame (David Kopf Instruments, Tujunga, CA, USA) on a heating pad.

For viral injections, the skull was exposed and a hole was drilled unilaterally above the target area. A 10 μl Hamilton syringe attached to a 31-gauge microinjection canula (AMI-5T, AgnTho's AB, Lidingö, Sweden) was used to administer the GFAP-G<sub>i</sub>-DREADD viral vector plasmid ssAAV-5/2-hGFAP-hm<sub>4</sub>D(Gi)\_mCherry-WPRE-hGHp(A) (physical titer:  $6.7 \times 10^{12}$  vg/ml) or the control plasmid pssAAV-5/2-hGFAP-EGFP-WPRE-hGHp(A) ( $1.8 \times 10^{13}$  vg/ml) (Viral Vector Facility of the Neuroscience Center Zurich, Zurich, Switzerland). The canula was gently lowered into the DLS (A/P: +0.5, M/L: -3.5 relative to bregma, V/D: -5.0 relative to skull; Paxinos and Watson 6<sup>th</sup> ed. 2007) and the solutions were infused using a microperfusion pump (Univentor-864 Syringe Pump; AgnTho's AB, Lidingö, Sweden). A total volume of 0.8 μl was infused at a flow rate of 0.05 μl/min. To allow for diffusion, the cannula was withdrawn 5 min after completion of the infusion. Rats were given postoperative analgesia (Norocarp, 5 mg/kg, s.c.) and returned to their home cage for three weeks prior to electrophysiology experiments or immunohistochemical verification.

For microdialysis experiments, the skull was exposed and one hole was drilled above the DLS unilaterally and two additional holes were drilled for attachment of anchoring screws. A custom made I-shaped probe, with a molecular cut-off of 20 kDa and an active space of 2 mm, was lowered into the brain using coordinates approximating DLS (A/P: +1.2, M/L: -3.5 relative to bregma; D/V: -5.5 relative to dura mater). The probe together with the two anchoring screws were fixed to the skull using Harvard cement (DAB Dental AB, Gothenburg, Sweden). Rats were housed individually and allowed to recover for 48 hours prior to the *in vivo* microdialysis experiment.

### *In vivo* microdialysis

*In vivo* microdialysis experiments were performed on awake and freely-moving rats as previously described [51]. In brief, the microdialysis probe was perfused with Ringer's solution at a rate of 2 μl/min for 2 h before baseline sampling was initiated. Samples were collected every 20 min. After obtaining four stable baseline samples, the metabolic uncoupler FC was perfused by reversed dialysis. Microdialysate dopamine content was analyzed using high-performance liquid chromatography with electrochemical detection, while amino acid content in the same sample were analyzed using fluorescent detection as previously described in detail [52]. As the effect of FC progressively increased over time, the  $t = 60$  min time-point was used for more in depth analysis. After the experiment, brains were fixed in accustain formaline-free fixative (Sigma-Aldrich) for 3–7 days

prior to verification of probe placement. Animals with misplaced probes or visual defects were excluded from the statistical analysis.

### Slice electrophysiology

**Brain slice preparations.** Coronal brain slices (250–300  $\mu\text{m}$ ), containing the striatum and the overlying cortex, were prepared from juvenile (<200 g) and young adult rats (>300 g) as previously described [53]. Slices were sectioned in ice-cold modified aCSF, consisting of (in mM): 220 sucrose, 2 KCl, 6  $\text{MgCl}_2$ , 26  $\text{NaHCO}_3$ , 1.3  $\text{NaH}_2\text{PO}_4$ , 0.2  $\text{CaCl}_2$ , and 10 D-glucose, and was allowed to equilibrate in normal aCSF at 30 °C for 30 min, and then in room temperature for the remainder of the day.

**Field potential recordings.** Field potential recordings were performed in DLS, as previously described [54]. In brief, one hemisphere of a brain slice was transferred to a recording chamber and continuously perfused with prewarmed aCSF (30 °C). Stimulating electrodes (TM33B, World Precision Instruments, FL, USA) were positioned close to the border between DLS and the overlying white matter, and population spikes (PS) were evoked with a paired pulse stimulation protocol (50 ms interpulse interval) at a frequency of 0.05 Hz. For recordings conducted in brain slices from rats receiving viral injections, the electrodes and recording pipette were located in proximity of the cannula track.

A stable baseline was monitored for at least ten minutes before drugs were administered via bath perfusion. Antagonists were perfused for at least 20 min prior to FC administration, and then continuously throughout the recording. Paired pulse ratio (PPR) was recorded for three minutes at the end both baseline and drug perfusion. Signals were amplified with a custom-made amplifier, filtered at 3 kHz, and digitized at 8 kHz. Responses with a half max PS amplitude smaller than 0.2 mV at baseline were excluded from analysis.

**Whole cell recordings.** Spontaneous excitatory and inhibitory postsynaptic currents (sEPSCs/sIPSCs) were recorded in medium spiny neurons (MSNs) voltage clamped at  $-65$  mV as previously described in detail [53]. In brief, recording pipettes (2.5–4.5 M $\Omega$ , borosilicate glass, Sutter Instruments) were filled with internal solution containing (in mM): 150 CsCl, 10 Hepes, 2  $\text{MgCl}_2$ , 0.3  $\text{Na}_2\text{GTP}$ , 3  $\text{MgATP}$ , and 0.2 BAPTA, with pH adjusted to 7.2 with CsOH, and osmolarity set to 298 mOsm with sucrose. To isolate sEPSCs, bicuculline (20  $\mu\text{M}$ ) was added to the prewarmed aCSF (32 °C), while sIPSCs were recorded in the presence of APV (50  $\mu\text{M}$ ) and CNQX (10  $\mu\text{M}$ ). A stable baseline was recorded for three minutes before drugs modulating astrocyte excitability (FC or CNO) were bath perfused. Whole cell recordings were conducted using an Axopatch 700B amplifier (Axon Instruments, Foster City, CA), filtered at 2 kHz, and digitized at 5 kHz (Digidata 1440 A, Axon Instruments). Data were acquired using Clampex 10.2 (Molecular Devices, San Jose, CA, USA). Only recordings with a stable series resistance that varied less than 20% and did not exceed 25 M $\Omega$  were included in the analysis.

### Immunohistochemistry

Animals were anesthetized with Allfatal vet. (100 mg/ml (pentobarbital); Omnidea AB, Stockholm, Sweden) and perfused transcardially with Tyrode's solution containing (in mM): 116 NaCl, 5.4 KCl, 1.6  $\text{MgCl}_2$ , 0.4  $\text{MgSO}_4$ , 1.3  $\text{NaH}_2\text{PO}_4$ , 26  $\text{NaHCO}_3$ , 5.5 glucose, followed by 4% ice-cold paraformaldehyde (PFA) solution. Brains were removed and post-fixed in 4% PFA followed by incubation in sucrose solutions (10% for 1 day followed by 20% for 7 days) before being snap frozen using isopentane on dry ice. Coronal slices (40  $\mu\text{m}$ ) were sectioned using a Leica CM1950 cryostat (Leica microsystems AB sections), placed in cryoprotective solution [30% glycerol, 30% ethylene glycol, 40% 1x Tris Buffered Saline (TBS: 0.15 M NaCl, 0.05 M Tris-HCl; pH 7.6)]. Brain sections were pretreated with 5% normal donkey serum (Jackson ImmunoResearch, West Grove, PA), and 0.1% triton-X-100 in TBS for 1 h, following incubation of primary antibodies targeting astrocytes (anti-GFAP (1:1000), Cat no: MA512023, Invitrogen, Thermo Fischer Scientific, Waltham, MA, USA) or neurons (anti-NeuN (1:400), Cat no: MABN140, Merck Millipore, Darmstadt, Germany) over night at 4 °C. Brain slices were washed in TBS prior to one-hour incubation with secondary antibodies (Alexa Flour 488 (1:1000), Cat no: A21202, Alexa Flour 647 (1:1000), Cat no: A31573, Invitrogen) diluted in TBS with 5% normal donkey serum and 0.1% triton X-100. A reporter molecule, mCherry, was fused to the construct coding for the DREADDs. Cells transfected with the virus were thus visualized in red. No further staining was used to verify the expression of the receptor. Brain sections were rinsed in TBS, mounted onto microscope slides using Fluoroshield (Merck, Darmstadt, Germany). Images were obtained using a Zeiss LSM 700 Inverted confocal

microscope (Zeiss, Jena, Germany), with a Plan-Apochromat 63x/1.40 objective (Zeiss, Germany).

### Statistics

Off-line analysis of electrophysiological recordings was performed using Clampfit 10.2 (Molecular Devices), MiniAnalysis 6.0 (Synaptosoft, Decatur, GA), Microsoft Excel (Redmond, WA), and GraphPad Prism 7 (GraphPad Software, San Diego, CA). Gaussian distribution was tested with D'Agostino–Pearson omnibus normality test. For analysis involving drug-perfusion, two-way analysis of variance (ANOVA) with a Bonferroni post hoc test was used for statistical analysis of treatment groups over time. Drug-induced effects on the microdialysate were calculated from  $t = 20$  min and for field potentials from  $t = 15$  minutes, until the end of drug-perfusion. Paired  $t$ -test was used for assessing absolute changes in microdialysate levels. For PPR analysis, paired  $t$ -test was applied, while whole cell recordings were assessed using two-way ANOVA, or paired  $t$ -test when applicable. Data are expressed as mean  $\pm$  SEM, and the level of significance was set to  $p < 0.05$ .

## RESULTS

### Inhibition of astrocytes alters the extracellular environment

The metabolic inhibitor FC (50  $\mu\text{M}$ ), which is preferentially taken up by glial cells [40], was administered using reversed dialysis. FC rapidly increased the extracellular levels of glutamate, and progressively decreased the levels of glutamine (two-way ANOVA <sub>$t = 20-180\text{min}$</sub> : glutamate: Time:  $F_{(8, 80)} = 2.22$ ,  $p = 0.034$ ; FC:  $F_{(1, 10)} = 45.6$ ,  $p < 0.001$ ; TimexFC:  $F_{(8, 80)} = 1.15$ ,  $p = 0.34$ ; glutamine: Time:  $F_{(8, 80)} = 19.7$ ,  $p < 0.001$ ;  $F_{(1, 10)} = 24.5$ ,  $p = 0.0006$ ; TimexFC:  $F_{(8, 80)} = 40.0$ ,  $p < 0.0001$ ) (Fig. 1B, D). An increase in glutamate from  $58 \pm 5.2$  to  $140 \pm 22$  nM ( $t_{(6)} = 4.09$ ,  $p = 0.006$ ; Fig. 1C) was observed after 60 minutes of FC administration in the dialysate, with a concomitant decline of extracellular glutamine ( $24 \pm 5.2$  to  $19 \pm 4.6$   $\mu\text{M}$ ;  $t_{(6)} = 3.31$ ,  $p = 0.016$ ; Fig. 1E).

The postulated inhibition of astrocytes by FC led to a long-lasting elevation of dopamine (Time:  $F_{(8, 80)} = 3.60$ ,  $p = 0.0013$ ; FC:  $F_{(1, 10)} = 10.4$ ,  $p = 0.009$ ; TimexFC:  $F_{(8, 80)} = 1.96$ ,  $p = 0.062$ ), where the microdialysate concentration of dopamine increased from  $6.9 \pm 1.0$  to  $10 \pm 1.9$  nM after 60 minutes of FC administration ( $t_{(6)} = 2.81$ ,  $p = 0.031$ ) (Fig. 1F–G). A trend towards a transient increase in taurine was observed in response to FC (Time:  $F_{(8, 80)} = 0.40$ ,  $p = 0.92$ ; FC:  $F_{(1, 10)} = 0.96$ ,  $p = 0.35$ ; TimexFC:  $F_{(8, 80)} = 0.48$ ,  $p = 0.87$ ), but this elevation was not significant at  $t = 60$  min (baseline level:  $740 \pm 94$  nM; 60 min FC:  $900 \pm 150$  nM;  $t_{(6)} = 2.23$ ,  $p = 0.067$ ) (Fig. 1H–J). The microdialysate level of serine was not affected (Time:  $F_{(8, 80)} = 1.12$ ,  $p = 0.36$ ; FC:  $F_{(1, 10)} = 0.19$ ,  $p = 0.67$ ; TimexFC:  $F_{(8, 80)} = 1.15$ ,  $p = 0.34$ ; baseline level:  $3.7 \pm 0.69$   $\mu\text{M}$ ; 60 min FC:  $4.10 \pm 0.82$   $\mu\text{M}$ ;  $t_{(6)} = 1.61$ ,  $p = 0.16$ ) (Fig. 1J, K), while an effect by time, but not FC, was seen when monitoring glycine levels (Time:  $F_{(8, 80)} = 4.18$ ,  $p = 0.0003$ ; FC:  $F_{(1, 10)} = 0.88$ ,  $p = 0.37$ ; TimexFC:  $F_{(8, 80)} = 0.91$ ,  $p = 0.52$ ; baseline level:  $1.1 \pm 0.14$   $\mu\text{M}$ ; 60 min FC:  $1.2 \pm 0.14$   $\mu\text{M}$ ;  $t_{(6)} = 2.21$ ,  $p = 0.069$ ) (Fig. 1L, M).

### Fluorocitrate suppresses excitatory neurotransmission

To further monitor FC-mediated effects on striatal neurotransmission, electrophysiological recordings were performed in acutely isolated brain slices. Following a stable baseline, FC (5  $\mu\text{M}$ ) was bath perfused. Continuous perfusion of FC decreased evoked field potentials (2 h perfusion: PS amplitude =  $55 \pm 5.8\%$  of baseline,  $t_{(19)} = 7.75$ ,  $p < 0.0001$ ) (data not shown). Since whole cell recordings are more easily assessed in juvenile rats, the response to FC was monitored in both juvenile rats (<200 g, 4–6 weeks old) and adults (>300 g, 9–12 weeks old, resembling the age for microdialysis). While FC produced a significant depression in slices from both juvenile and adult animals (FC:  $F_{(2, 61)} = 17.6$ ,  $p < 0.001$ ; post hoc analysis: aCSF vs FC juvenile:  $q_{(61)} = 5.05$ ,  $p = 0.002$ ; aCSF vs FC adult:  $q_{(61)} = 8.25$ ,  $p < 0.001$ ) (Fig. 2B), synaptic depression in brain slices from adult rats showed a faster onset of depression ( $t = 15-70$ :  $F_{(1, 38)} = 40$ ,  $p < 0.0001$ ) (Fig. 2B). In addition, only brain



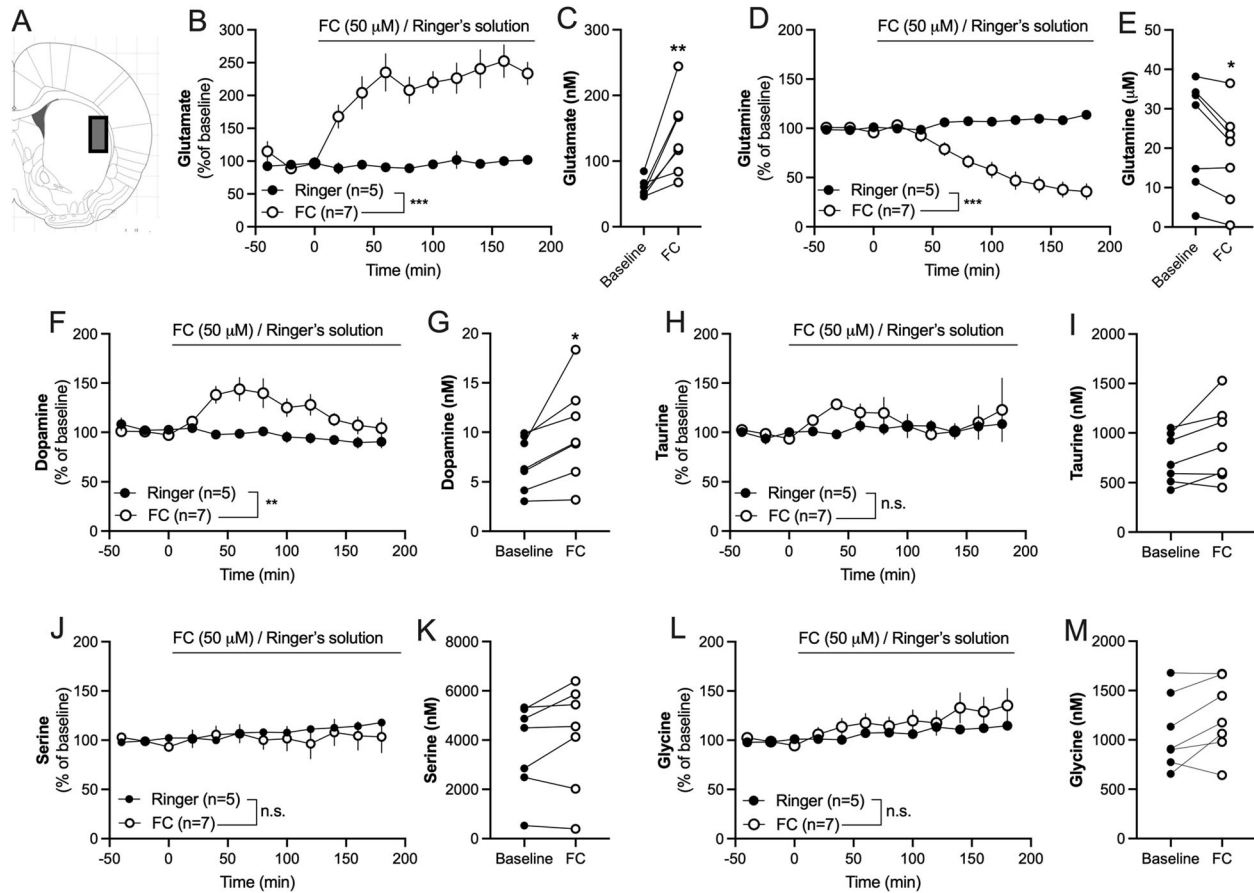


**Fig. 1 Inhibition of astrocytes alters the extracellular environment.** **A** Histological representation with a rectangle marking the region for microdialysis perfusion and sampling. **B** Administration of fluorocitrate (FC, 50  $\mu\text{M}$ ) via the microdialysis probe produced a sustained elevation of extracellular glutamate levels as compared to Ringer-treated control. **C** Graph demonstrates the microdialysate concentration of glutamate in individual animals at baseline and after 60 min perfusion with FC. **D** Continuous administration of FC progressively reduced glutamate levels. **E** Graph demonstrates the microdialysate concentration of glutamine in individual animals at baseline and after 60 min FC perfusion. **F–I** Administration of FC via the microdialysis probe increased dopamine levels, and transiently elevated extrasynaptic taurine. **J–M** The amino acids serine and glycine were not significantly altered by FC. Time course graphs show relative values  $\pm$  SEM. Individual data correspond to microdialysate concentration at baseline and following 60 min of FC administration.  $n$  = number of rats. \* $p$  < 0.05, \*\* $p$  < 0.01, \*\*\* $p$  < 0.001.

slices from older animals showed restored neurotransmission in response to FC wash-out (juvenile vs. adult,  $t = 80\text{--}130$ :  $F_{(1, 38)} = 4.79$ ,  $p = 0.035$ ) (Fig. 2B). FC increased PPR in both juvenile and adult animals (<200 g:  $t_{(15)} = 2.63$ ,  $p = 0.019$ ; >300 g:  $t_{(13)} = 3.70$ ,  $p = 0.0027$ ), indicating that FC suppresses PS amplitude by reducing the probability of transmitter release (Fig. 2C). To more specifically outline changes in excitatory transmission, whole cell recordings were performed and sEPSCs monitored during continuous perfusion of bicuculline (20  $\mu\text{M}$ ) with or without FC. FC significantly depressed sEPSC frequency ( $t_{(5)} = 5.71$ ,  $p = 0.002$ ), and reduced sEPSC amplitude ( $t_{(5)} = 4.38$ ,  $p = 0.007$ ), while rise and decay time remained unaffected (rise-time:  $t_{(5)} = 1.82$ ,  $p = 0.13$ ; decay-time:  $t_{(5)} = 1.52$ ,  $p = 0.19$ ) (Fig. 2E–G).

Astrocytes are also important for GABAergic neurotransmission, and reduced glutamine levels may in the extension lead to impaired inhibitory signaling. To assess transformations in inhibitory transmission, a second set of experiments was performed, where brain slices were incubated in FC for at least five hours before electrophysiological recordings were conducted. Extended incubation of FC significantly suppressed the frequency of inhibitory inputs when compared to aCSF-treated control (sIPSC frequency:  $t_{(9)} = 2.52$ ,  $p = 0.033$ ; amplitude:  $t_{(9)} = 1.09$ ,  $p = 0.31$ ; rise-time:  $t_{(9)} = 0.41$ ,  $p = 0.70$ ; decay-time:  $t_{(9)} = 0.74$ ,  $p = 0.48$ ) (Fig. 2H–I), suggesting that extended inhibition of astrocytes also suppresses inhibitory neurotransmission.

### G<sub>i</sub>-coupled DREADDs targeting GFAP in DLS selectively suppress the frequency of excitatory inputs to MSNs

To further confirm that the effects monitored in response to FC-treatment are attributed to inhibition of astrocytes, G<sub>i</sub>-coupled DREADDs were selectively expressed in GFAP-expressing astrocytes as previously shown by others [55, 56] (Fig. 3A). Following three weeks of incubation, immunohistological staining showed that G<sub>i</sub>-coupled DREADDs were expressed along the site of injection (Fig. 3B), and associated with GFAP (Fig. 3J–N). Expression of DREADDs could also be found in a few cells in cortical tissue, indicating a slight spread through gap junction channels (Fig. 3B) [37]. Bath perfusion of the DREADDs agonist CNO (10  $\mu\text{M}$ ) revealed a differential effect on the frequency of recorded sEPSCs as compared to sIPSCs (Fig. 3C). While excitatory neurotransmission was significantly depressed by CNO in slices expressing G<sub>i</sub>-coupled DREADDs, there was a trend towards an enhanced frequency of sIPSCs following CNO administration (CNO:  $F_{(2, 25)} = 7.05$ ,  $p = 0.0037$ ; post hoc analysis: sEPSC vs. sIPSC:  $q_{(25)} = 5.31$ ,  $p = 0.0026$ ; sEPSC control vs. sEPSC DREADDs:  $q_{(25)} = 3.55$ ,  $p = 0.048$ ; sIPSC control vs. sIPSC DREADDs:  $q_{(25)} = 2.60$ ,  $p = 0.18$ ) (Fig. 3C). Both excitatory and inhibitory amplitudes remained unaffected by CNO administration in slices expressing inhibitory DREADDs (sIPSC amplitude at  $t = 15\text{--}20$  min =  $100 \pm 4.4\%$  of baseline,  $t_{(8)} = 0.03$ ,  $p = 0.98$ ; sEPSC amplitude at  $t = 15\text{--}20$  min =  $99 \pm 4.3\%$  of baseline,  $t_{(4)} = 0.16$ ,  $p = 0.89$ ) (Fig. 3D).

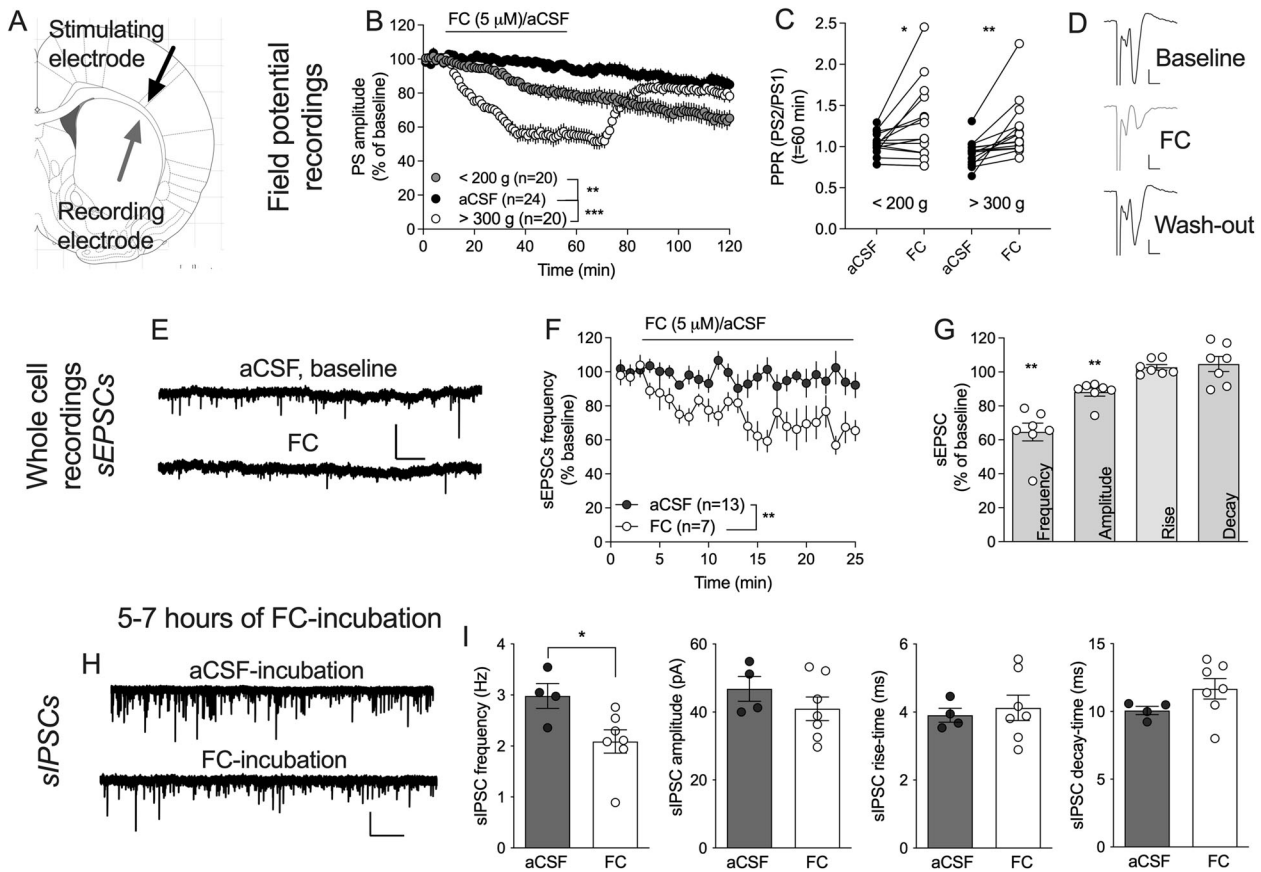


**Fig. 2 Fluorocitrate suppresses striatal neurotransmission.** **A** Schematic drawing showing the position of recording (gray) and stimulating (black) electrodes for field potential recordings. **B** Synaptic depression induced by FC was partially age-dependent. **C** PPR was significantly increased by FC in slices from both juvenile and adult rat brains. **D** Example traces show evoked PSs at baseline (black), after 60 min of FC-perfusion (gray), and 60 min drug washout (black) in a brain slice from an adult rat. Calibration: 0.2 mV, 2 ms. **E** Example traces showing recorded sEPSCs at baseline (aCSF) and after 20 min perfusion of FC (5  $\mu$ M). Calibration: 50 pA, 5 s. **F** Time course graph showing recorded sEPSC frequency during perfusion of FC or aCSF. **G** Bar graph shows relative change in sEPSCs after 20 min of FC administration. **H** Example traces showing inhibitory neurotransmission following five hours of incubation in aCSF (control) or FC. Calibration: 100 pA, 10 s. **I** Extended incubation in FC resulted in a reduced frequency of inhibitory inputs to striatal MSNs, while postsynaptic sIPSC parameters were not significantly modulated. Data are presented as mean values  $\pm$  SEM and based on at least five rats/group. n=number of recordings. \*\* $p < 0.01$ , \*\*\* $p < 0.001$ .

When monitoring the response to CNO (10  $\mu$ M) in field potential recordings, PS amplitude was significantly depressed in slices expressing inhibitory DREADDs in astrocytes, as compared to slices from rats injected with the empty plasmid ( $F_{(1, 43)} = 42$ ,  $p < 0.001$ ) (Fig. 3E). However, a slight depression of PS amplitude was also apparent in slices from animals injected with the empty plasmid ( $F_{(1, 42)} = 5.40$ ,  $p = 0.025$ ). Similarly, CNO perfusion significantly increased PPR in both control ( $t_{(8)} = 2.72$ ,  $p = 0.026$ ) and DREADDs expressing slices ( $t_{(7)} = 4.54$ ,  $p = 0.003$ ), indicating that CNO, at the concentration used, slightly reduced the probability of transmitter release (Fig. 3F). The relative change in PPR, however, was significantly greater in DREADDs-expressing slices ( $t_{(15)} = 2.84$ ,  $p = 0.013$ ). A lower concentration of CNO (2  $\mu$ M), which did not significantly affect PS amplitude by itself ( $F_{(1, 17)} = 0.28$ ,  $p = 0.61$ ), selectively reduced PS amplitude ( $F_{(1, 26)} = 6.87$ ,  $p = 0.014$ ) and increased PPR ( $t_{(19)} = 2.89$ ,  $p = 0.0098$ ) in slices transfected with  $G_i$ -coupled DREADDs (Fig. 3G, H).

#### Synaptic depression induced by fluorocitrate is not connected to glutamatergic autoreceptors

In vivo microdialysis revealed a robust increase in the extracellular levels of glutamate, with a concomitant decrease in extracellular glutamine. To determine if reduced glutamine could contribute to reduced probability of transmitter release, brain slices were

pretreated with glutamine (1 mM) prior to co-perfusion with FC (5  $\mu$ M). Glutamine did not alter PS amplitude by itself ( $F_{(1, 29)} = 1.12$ ,  $p = 0.30$ ) (data not shown), and did not prevent synaptic depression elicited by FC ( $F_{(1, 35)} = 8.75$ ,  $p = 0.0055$ , PPR:  $t_{(19)} = 4.39$ ,  $p < 0.001$ ) (Fig. 4A, B). Increased extracellular levels of glutamate may also decrease the probability of transmitter release by activating extrasynaptic autoreceptors. Notably, pre-treatment with neither the mGluR2/3 inhibitor LY 341495 (200 nM) ( $F_{(1, 51)} = 21.2$ ,  $p < 0.001$ ), nor the NMDA receptor antagonist APV (50  $\mu$ M) ( $F_{(1, 54)} = 13.1$ ,  $p < 0.001$ ), was sufficient to prevent FC-mediated depression (Fig. 4B), or to block the increase in PPR mediated by FC (LY 341495 + FC:  $t_{(23)} = 5.20$ ,  $p < 0.001$ ; APV + FC:  $t_{(14)} = 2.32$ ,  $p = 0.036$ ) (Fig. 4B, C).

Increased extrasynaptic glutamate may also suppress the probability of transmitter release by activating other signaling pathways, including by increasing the release of endogenous endocannabinoids, GABA or opioids [57, 58]. But, FC-induced depression was insensitive to inhibitors targeting endocannabinoid activated cannabinoid 1 receptors (AM251 (2  $\mu$ M):  $F_{(1, 32)} = 8.78$ ,  $p = 0.0057$ ; PPR:  $t_{(23)} = 2.64$ ,  $p = 0.015$ ), GABA<sub>A</sub> receptors (bicuculline (20  $\mu$ M):  $F_{(1, 44)} = 16.0$ ,  $p < 0.001$ ; PPR:  $t_{(12)} = 3.25$ ,  $p = 0.007$ ); or  $\mu$ -opioid receptors (CTAP (50 nM):  $F_{(1, 15)} = 39.5$ ,  $p < 0.001$ ) (Fig. 4E). FC-mediated depression was also insensitive to inhibition of the astroglial syncytium using the gap junction

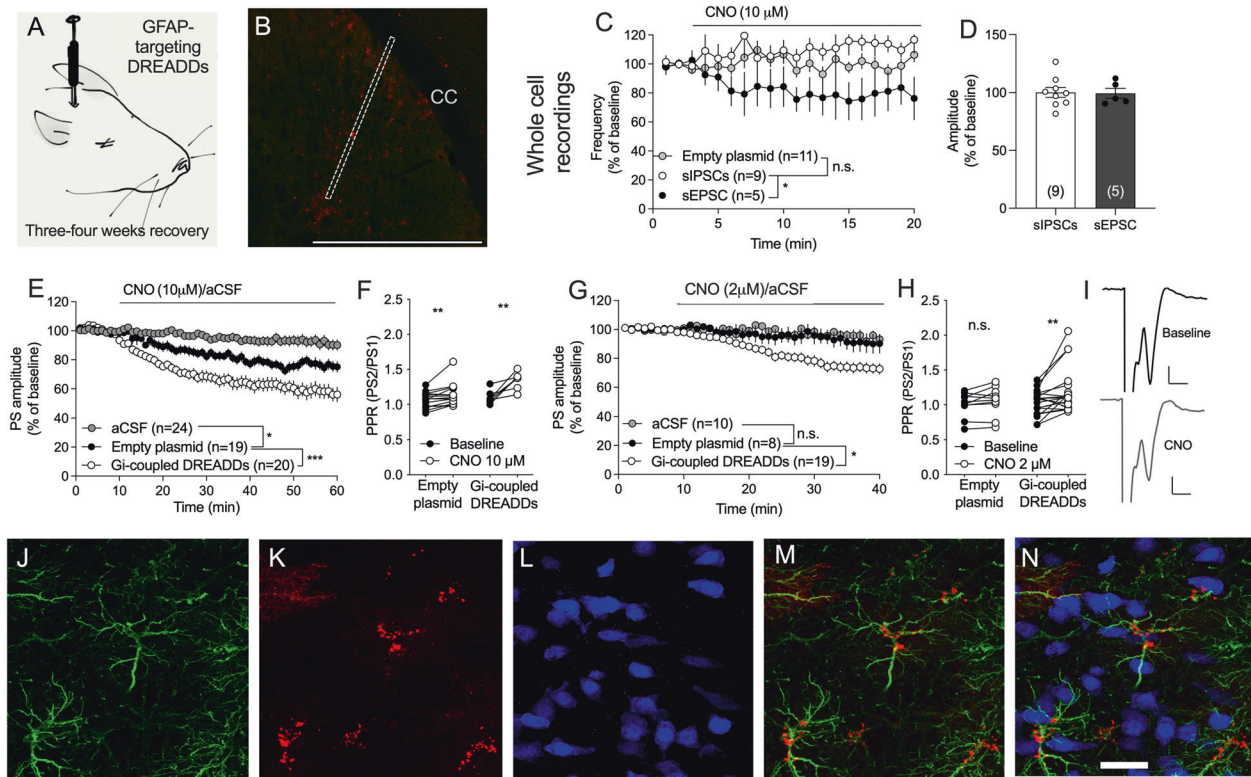


**Fig. 3** Activation of  $G_i$ -coupled DREADDs targeting GFAP selectively suppresses excitatory neurotransmission. **A** AAV containing  $G_i$ -coupled DREADDs targeting GFAP was injected into the DLS, and rats were left to recover for at least three weeks before slice electrophysiology was conducted. **B** Viral transfection of the DREADDs virus was visualized with mCherry (red). Dotted line marks the approximate position of the cannula track. Note that viral transfection is not strictly restricted to the injection site. Calibration: 1 mm. CC corpus callosum. **C** Whole cell recordings showed a trend towards differential effect on inhibitory and excitatory currents, where CNO ( $10 \mu\text{M}$ ) selectively depressed the frequency of excitatory inputs to striatal MSNs. **D** CNO showed no effect on spontaneous current amplitudes. **E** When monitoring evoked field potentials, CNO ( $10 \mu\text{M}$ ) significantly depressed PS amplitude in slices expressing inhibitory DREADDs as compared to slices expressing the empty plasmid. There was, however, also a slight depression of evoked potentials by CNO itself. **F** The decrease in PS amplitude elicited by CNO coincided with an increase in PPR. **G, H** A lower concentration of CNO ( $2 \mu\text{M}$ ) selectively suppressed evoked potentials in brain slices from rats transfected with  $G_i$ -coupled DREADDs as compared to empty plasmid. **I** Example traces showing evoked PS amplitudes at baseline (black) and after CNO ( $2 \mu\text{M}$ ) administration (gray). **J** Viral transfection indicating DREADDs expression visualized with mCherry. **K** Immunohistochemical staining showing GFAP-expressing astrocytes. **L** Neurons visualized by NeuN. **M, N** Overlay of figure (J) and (K) (M), or J, K and L (N) demonstrates that viral transfection is associated with GFAP-expressing cells. Calibration:  $20 \mu\text{m}$ . Data are based on at least four animals/treatment and presented as mean values  $\pm$  SEM. n number of recordings. \* $p < 0.05$ , \*\* $p < 0.01$ .

inhibitor carbenoxolone ( $100 \mu\text{M}$ ;  $F_{(1, 20)} = 73$ ,  $p < 0.001$ ), or when reducing gliotransmitter signaling by bath perfusion of the non-selective P2 antagonist PPADS ( $F_{(1, 22)} = 38$ ,  $p < 0.001$ ) (Fig. 4D, E). It should be noted, that both carbenoxolone ( $F_{(1, 22)} = 38$ ,  $p < 0.001$ ) as well as PPADS ( $F_{(1, 30)} = 12$ ,  $p = 0.002$ ), suppressed PS amplitude by themselves, but that FC further reduced synaptic output from drug-treated baseline (Fig. 4D).

#### Dopamine D2 receptor signaling contributes to synaptic depression mediated by fluorocitrate

Astrocytes have been implicated as important modulators of dopamine transmission, and in vivo microdialysis demonstrated increased dopamine levels following FC administration. To assess the role of dopamine signaling on FC-mediated depression, slices were pre-treated with a cocktail containing the dopamine D1 receptor antagonist SCH23390 ( $0.5 \mu\text{M}$ ) and the dopamine D2 receptor antagonist sulpiride ( $5 \mu\text{M}$ ). The combination of antagonists blocked the depression mediated by FC ( $F_{(1, 49)} = 20.9$ ,  $p < 0.001$ ) (Fig. 4G). Pre-treatment with SCH23390 alone did not affect FC-mediated depression (FC vs. SCH23390 + FC:  $F_{(1, 10)} = 2.44$ ,  $p = 0.15$ ), but incubation with sulpiride was sufficient to suppress synaptic depression induced by FC (FC vs. sulpiride + FC:  $F_{(1, 42)} = 17.4$ ,  $p < 0.001$ ) (Fig. 4G). The inhibition was not significantly stronger when using the cocktail as compared to sulpiride alone

(post hoc analysis:  $q_{(1145)} = 1.51$ ,  $p = 0.54$ ) (Fig. 4G). FC increased PPR in slices pre-treated with SCH23390 ( $t_{(9)} = 5.24$ ,  $p < 0.001$ ) or SCH23390 in combination with sulpiride ( $t_{(22)} = 2.97$ ,  $p = 0.007$ ) (Fig. 4I), but not in slices incubated in sulpiride alone ( $t_{(20)} = 0.74$ ,  $p = 0.47$ ) (Fig. 4I). PS amplitude was not modulated by sulpiride perfusion ( $F_{(1, 10)} = 0.14$ ,  $p = 0.71$ ) (data not shown).

In vivo microdialysis revealed a robust increase in the extracellular levels of glutamate indicative of impaired clearance through glial glutamate transporters GLT-1 and GLAST. In the last set of experiments slices were treated with a low concentration of TFB-TBOA ( $200 \text{ nM}$ ), which should selectively inhibit GLT-1 and GLAST. Similar to FC, administration of TFB-TBOA significantly depressed PS amplitude ( $F_{(1, 34)} = 21$ ,  $p < 0.001$ ) (Fig. 4H), and increased PPR ( $t_{(21)} = 3.52$ ,  $p = 0.002$ ) (Fig. 4J), suggesting that reduced glutamate uptake/increased extracellular glutamate levels partially underlies FC-mediated depression of striatal output. To further outline the role of dopamine D2 receptor signaling, brain slices were then pre-treated with sulpiride prior to administration of the glial glutamate transporter inhibitor TFB-TBOA. Similar to FC-mediated depression, sulpiride inhibited synaptic depression induced by TFB-TBOA as compared to aCSF-treated control ( $F_{(1, 42)} = 24.0$ ,  $p < 0.001$ ) (Fig. 4H). However, even though sulpiride+TFB-TBOA was insufficient to depress PS amplitude when compared to aCSF perfusion ( $F_{(1, 43)} = 3.25$ ,  $p =$



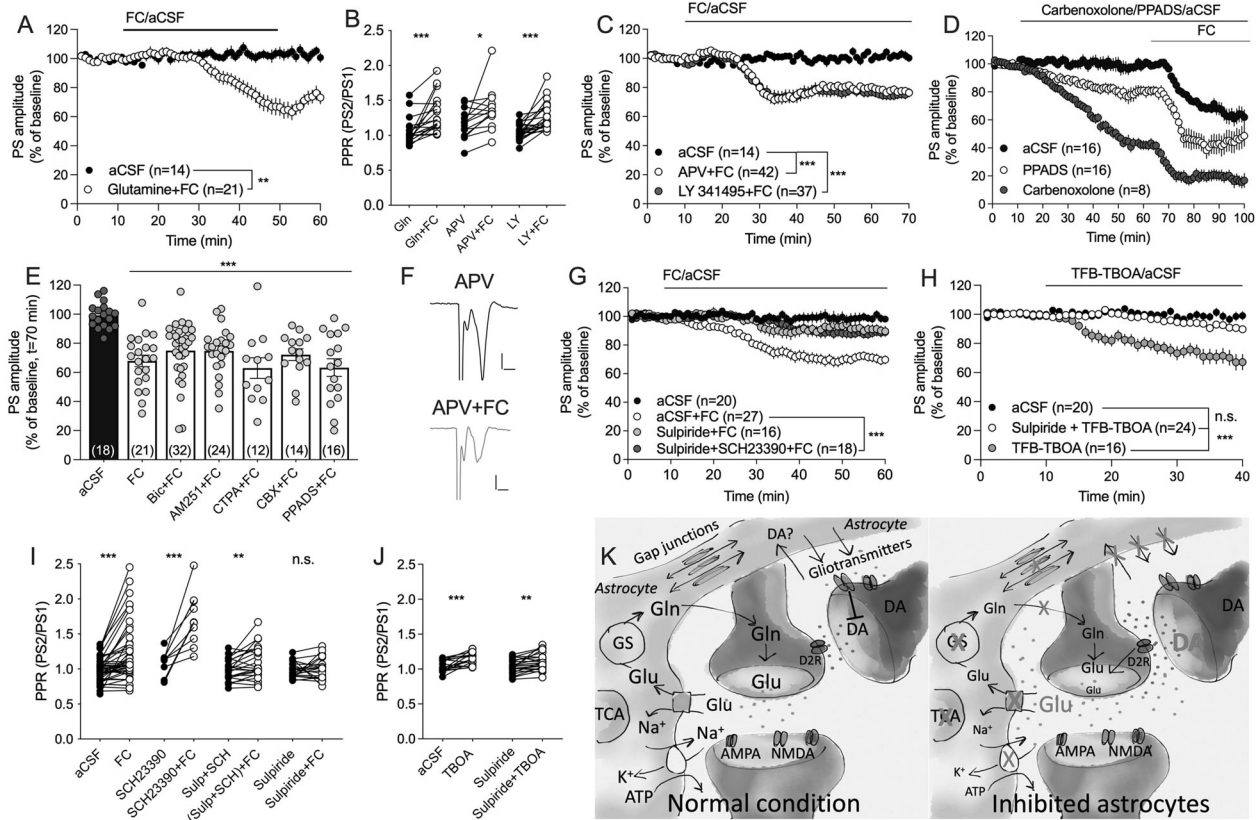


**Fig. 4 Dopamine D2 receptors are involved in FC-mediated depression of synaptic output.** **A** Co-administration of glutamine was not sufficient to prevent synaptic depression mediated by FC. **B** Depression of PS amplitude was accompanied by increased PPR, indicative of reduced probability of transmitter release. **C** Inhibition of glutamate receptors using the NMDA receptor antagonist APV, or the mGluR2/3 antagonist LY 341495, was insufficient to block FC-mediated depression of evoked potentials. **D** Carbenoxolone and PPADS depressed PS amplitude by themselves, but did not prevent FC-mediated depression. **E** Pre-treatment with antagonists targeting GABA<sub>A</sub> receptors (Bic), cannabinoid 1 receptors (AM251),  $\mu$ -opioid receptors (CTAP), gap junction coupling (carbenoxolone, CBX), or purinergic P2 receptors (PPADS), were insufficient to block FC-mediated depression. **F** Example traces showing evoked PSs during APV-treated baseline (black) and following APV + FC perfusion (gray). Calibration: 0.2 mV, 2 ms. **G** Pre-treatment with a cocktail of the dopamine D1 and D2 receptor antagonists SCH23390 and sulpiride inhibited synaptic depression mediated by FC, as did sulpiride pre-treatment alone. **H** A low concentration of the glutamate transporter inhibitor TFB-TBOA, which should act selectively on astrocytic glutamate uptake, significantly depressed PS amplitude in a manner blocked by sulpiride. **I** While FC was insufficient to increase PPR in slices pretreated in sulpiride, the effect was still present in slices incubated in a cocktail of sulpiride and SCH23390. **J** TFB-TBOA significantly increased PPR in both control slices, and in slices pre-treated with sulpiride. Data are based on at least four animals/treatment and presented as mean values  $\pm$  SEM. n number of recordings. \* $p < 0.05$ , \*\* $p < 0.01$ , \*\*\* $p < 0.001$ . **K** Schematic drawing showing how a reduced activity of astrocytes might result in decreased probability of transmitter release. Metabolic inhibition of astrocytes reduces ATP levels and GS function, and will lead to reduced uptake of glutamate, potassium, and possibly also dopamine. Fluorocitrate also impairs astrocyte calcium signaling, resulting in reduced release of gliotransmitters, including the endogenous antagonist kynurenic acid. These changes will lead to elevated levels of glutamate and dopamine in the extracellular space, and activation of dopamine D2 receptors, which will act to further suppress glutamate release. TCA tricarboxylic acid cycle, GS glutamine synthetase, Gln glutamine, Glu glutamate, DA dopamine.

0.079), PPR was still enhanced ( $t_{(22)} = 3.58$ ,  $p = 0.0017$ ) (Fig. 4J), indicating that the probability of transmitter release is reduced also during dopamine D2 receptor blockade.

## DISCUSSION

By employing a battery of neurobiological techniques, the data presented here support a role for astrocytes in modulating striatal neurotransmission. Metabolic inhibition of astrocytes in the DLS increased and decreased extracellular glutamate and glutamine levels, respectively, and suppressed synaptic output through mechanisms involving dopamine D2 receptor activation. The suppressed synaptic output following metabolic inhibition of astrocytes was confirmed in experiments where G<sub>i</sub>-coupled DREADDs targeting GFAP was activated, and in brain slices where astroglial glutamate-transporters GLAST and GLT-1 were blocked. While excitatory neurotransmission was especially compromised in the initial step, longer incubation of FC also suppressed

inhibitory neurotransmission, supporting a role for astrocytes in sustaining striatal neurotransmission [59].

Fluorocitrate, which is preferentially taken up by glial cells, inhibits the Krebs cycle and should putatively render the tissue devoid of metabolically active astrocytes [40, 60, 61]. Considering the role of astrocytes in clearing glutamate from the extracellular space and releasing glutamine [17], a differential effect on these amino acids would be expected if FC impairs astrocyte function. In support of this notion, we found that continuous administration of FC via the microdialysis probe rapidly increased the extracellular levels of glutamate, while progressively decreasing glutamine levels over time. Even though other cells also might be affected, these findings support a robust inhibition of striatal astrocytes by FC [7]. Interestingly, even though astrocytes have been acknowledged for regulating glycine and serine levels [8, 62, 63], neither glycine nor serine levels were altered following local administration of 50  $\mu$ M FC via the microdialysis probe. A higher concentration of FC (0.5 mM) has previously been shown to slightly reduce

D-serine levels in the medial prefrontal cortex, while still having no effect on extrasynaptic glycine levels [64]. At the same time, FC produces a massive increase in glycine levels when administered in the substantia nigra [65], suggesting that glycine uptake may be brain region specific.

Even though the microdialysate concentration of glutamate was increased by FC, both evoked field potentials as well as the frequency of spontaneous excitatory currents were depressed, suggesting that FC reduces the probability of glutamate release. Importantly, the decrease in PS amplitude induced by FC was mimicked not only by activating  $G_i$ -coupled DREADDs targeting GFAP, but also by the glial glutamate transporter inhibitor TFB-TBOA, collectively suggesting that impaired astrocyte function results in suppressed synaptic output. Astrocytic glutamate uptake is important for maintaining spatial and temporal specificity of synaptic transmission, and the conversion of glutamate by glutamine synthase is fundamental to ensure an efficient clearance of glutamate to prevent glutamate spillover [66]. Fluorocitrate may thus depress PS amplitude by activating extrasynaptic autoreceptors, or via receptor desensitization. However, inhibition of glutamate receptors, including mGluR2/3 and NMDAR, were insufficient to prevent FC-mediated depression. Importantly, the enhanced glutamate levels in the microdialysis following FC treatment most likely reflect non-synaptic, "metabolic" glutamate, and appear in lower concentrations than what is required for activation of synaptically located glutamatergic receptors and possibly also for autoreceptors [67]. Another possible explanation to the reduced PS amplitudes observed is that all three manipulations (FC, TFB-TBOA, and CNO treatment of DREADDs-expressing cells) probably reduce substrate presentation (glutamine), thereby decreasing glutamate synthesis and in the extension also synaptic transmission [68, 69]. However, co-perfusion of glutamate together with FC was not sufficient to prevent synaptic depression.

In adult rats, neurotransmission partially recovered after FC washout, suggesting that the effect by FC in this experimental set up to some extent is reversible. In contrast, in juvenile rats the onset of the FC-mediated effects on neurotransmission was slower and there was no recovery in response to drug-washout. These findings might be explained by age-related changes in glutamate clearance. Studies performed in other brain regions have shown an age-dependent upregulation of glutamate transporters [70], and the level of extracellular glutamate in cortex may be up to three times higher in rats weighing below 200 g as compared to rats >300 g [71]. If true also in the striatum, the more rapid onset in brain slices from adult animals could be connected to a more active control over excitatory transmission. The delayed recovery may partially also be explained by higher extrasynaptic glutamate levels and slower glutamate clearance as astrocytes recover from inhibition.

Astrocytes have previously been implicated in modulating dopamine transmission, possibly via the osmoregulatory amino acid taurine [72, 73] or by regulating GABA transporter activity [74]. Reversed dialysis of FC in the DLS increased extracellular levels of taurine, which in turn may elicit striatal dopamine release through an interaction with glycine receptors [75]. Whether the release of taurine is secondary to osmotic phenomena in response to the FC perfusion or directly linked to inhibition of astrocyte function, remains to be determined. It also remains to be determined if the increase in dopamine is secondary to elevated levels of taurine or glutamate, or more directly associated with FC administration and/or impaired astrocyte function. One possible mechanism involves kynurenic acid, a neuroactive substance that is synthesized by astrocytes. In fact, intra-striatal administration of FC has been shown to reversibly suppress the extracellular level of kynurenic acid, while in parallel increasing the microdialysate of dopamine [76]. Furthermore, inhibition of kynurenic acid synthesis alone is sufficient to increase extracellular dopamine [76]. It is thus

possible that the release of kynurenic acid from astrocytes produces a tonic inhibitor over dopaminergic neurons, which is released in response to FC administration. Astrocytes may also regulate extracellular dopamine levels by directly transporting and metabolizing dopamine [72], a function that may be compromised by FC. Interestingly, glutamine increases in response to dopaminergic lesion [77], and decreases when dopamine is high through mechanisms involving dopamine D2 receptor signaling [78]. Dopamine signaling may thus be key in astrocyte-neuronal crosstalk, which is also supported by studies conducted in other striatal subregions [27].

The dopamine D2 receptor antagonist sulpiride partially reduced the effect by FC on synaptic output. Sulpiride also blocked synaptic depression produced by the glutamate transporter inhibitor TFB-TBOA. Whether these dopamine D2 receptors are located on presynaptic neuronal terminals, interneurons, astrocytes or MSNs remains to be established. Collectively, these findings suggest that impaired astrocyte function results in elevated dopamine levels, which in turn suppresses neuronal activity via inhibitory dopamine D2 receptors. The increase in extracellular glutamate may contribute by producing neuronal depolarization, which decreases dopamine affinity at dopamine D1-like receptors thereby promoting inhibition via dopamine D2 receptors [79]. Altogether, considering that dopamine-signaling is pivotal for both structural and synaptic plasticity [80–82], increased dopamine signaling produced by impaired astrocyte function may result in a long-lasting transformation of striatal neurotransmission.

There is evidence that the metabolic uncoupler FC acts selectively on astrocytes [40, 41], and a robust impairment of astrocytic function by this compound with simultaneous sparing of neuronal function is also supported by our microdialysis data (glutamate/glutamine and dopamine data, respectively). However, it is still possible that parts of the results are linked to unspecific effects on neurons. Likewise, even though TFB-TBOA should block GLAST and GLT-1, the specificity regarding the location of these receptors may be questioned [14]. At the same time, in our hands, inhibition of the astrocytic syncytium using carbenoxolone, or blocking gliotransmission using PPADS, also depressed evoked PS amplitudes. Thus, all compounds applied to reduce astrocyte function produced similar effects on synaptic transmission, and these effects were mimicked in experiments where CNO was used to activate  $G_i$ -coupled DREADDs targeting GFAP. However, it should be noted that similar results as presented here also have been shown during activation of  $G_q$ -coupled DREADDs targeting GFAP *ex vivo* [27]. Even though the latter experiments were conducted using a high concentration of CNO (1 mM), which in our hands has a depressant effect on control slices, these results highlight the fact that it may be difficult to regulate astrocyte activity via G-protein coupled receptors [83]. In fact, both astrocytic  $G_q$  and  $G_{i/o}$  DREADD activation has been shown to increase neuronal action potential firing in the hippocampus [84]. Furthermore, experiments conducted in the dorsomedial striatum suggest that astrocyte may regulate the activity of medium spiny neurons in a pathway-specific manner [85]. Interestingly, the depressant effect by CNO was more pronounced in field potential recordings. This might be linked to the fact that responses are evoked instead of spontaneous, or that a collective response from many neurons is monitored. Even if the effect by 10  $\mu$ M CNO is minor, the effect may be more pronounced if all neurons respond in the same direction.

Taken together, even though astrocytes may be difficult to disentangle from neurons, the data presented here collectively support the hypothesis that astrocytes tonically modulate striatal neurotransmission. Furthermore, the effects observed on excitatory neurotransmission following inhibition of astrocyte function were antagonized by dopamine D2 receptor blockade, suggesting that the dopaminergic system is recruited during astrocyte-neuronal communication [27].



## REFERENCES

1. Rossi D. Astrocyte physiopathology: At the crossroads of intercellular networking, inflammation and cell death. *Prog Neurobiol.* 2015;130:86–120.
2. Halassa MM, Fellin T, Takano H, Dong JH, Haydon PG. Synaptic islands defined by the territory of a single astrocyte. *J Neurosci: Off J Soc Neurosci.* 2007;27:6473–7.
3. Bergles DE, Jabs R, Steinhauser C. Neuron-glia synapses in the brain. *Brain Res Rev.* 2010;63:130–7.
4. Bushong EA, Martone ME, Jones YZ, Ellisman MH. Protoplasmic astrocytes in CA1 stratum radiatum occupy separate anatomical domains. *J Neurosci: Off J Soc Neurosci.* 2002;22:183–92.
5. Covelo A, Araque A. Lateral regulation of synaptic transmission by astrocytes. *Neuroscience* 2016;323:62–6.
6. Wilton DK, Dissing-Olesen L, Stevens B. Neuron-glia signaling in synapse elimination. *Annu Rev Neurosci.* 2019;42:107–27.
7. Adermark L, Bowers MS. Disentangling the role of astrocytes in alcohol use disorder. *Alcohol, Clin Exp Res.* 2016;40:1802–16.
8. Henneberger C, Papouin T, Oliet SH, Rusakov DA. Long-term potentiation depends on release of D-serine from astrocytes. *Nature* 2010;463:232–6.
9. Martin R, Bajo-Graneras R, Moratalla R, Perea G, Araque A. Circuit-specific signaling in astrocyte-neuron networks in basal ganglia pathways. *Science* 2015;349:730–4.
10. Perea G, Araque A. Properties of synaptically evoked astrocyte calcium signal reveal synaptic information processing by astrocytes. *J Neurosci.* 2005;25:2192–203.
11. Perea G, Sur M, Araque A. Neuron-glia networks: integral gear of brain function. *Front Cell Neurosci.* 2014;8:378.
12. Cresto N, Pillet LE, Billuart P, Rouach N. Do astrocytes play a role in intellectual disabilities? *Trends Neurosci.* 2019;42:518–27.
13. Blanco-Suarez E, Caldwell AL, Allen NJ. Role of astrocyte-synapse interactions in CNS disorders. *J Physiol.* 2017;595:1903–16.
14. Zhou Y, Danbolt NC. GABA and glutamate transporters in brain. *Front Endocrinol (Lausanne).* 2013;4:165.
15. Kanner BI, Schuldiner S. Mechanism of transport and storage of neurotransmitters. *CRC Crit Rev Biochem.* 1987;22:1–38.
16. Karlsson RM, Tanaka K, Heilig M, Holmes A. Loss of glial glutamate and aspartate transporter (excitatory amino acid transporter 1) causes locomotor hyperactivity and exaggerated responses to psychotomimetics: rescue by haloperidol and metabotropic glutamate 2/3 agonist. *Biol Psychiatry.* 2008;64:810–4.
17. Hayashi MK. Structure-function relationship of transporters in the glutamate-glutamine cycle of the central nervous system. *Int J Mol Sci.* 2018;19:1177.
18. Faideau M, Kim J, Cormier K, Gilmore R, Welch M, Auregan G, et al. In vivo expression of polyglutamine-expanded huntingtin by mouse striatal astrocytes impairs glutamate transport: a correlation with Huntington's disease subjects. *Hum Mol Genet.* 2010;19:3053–67.
19. Hassel B, Tessler S, Faull RL, Emson PC. Glutamate uptake is reduced in prefrontal cortex in Huntington's disease. *Neurochem Res.* 2008;33:232–7.
20. Roberts-Wolfe DJ, Kalivas PW. Glutamate transporter GLT-1 as a therapeutic target for substance use disorders. *CNS Neurol Disord Drug Targets.* 2015;14:745–56.
21. Karlsson RM, Adermark L, Molander A, Perreau-Lenz S, Singley E, Solomon M, et al. Reduced alcohol intake and reward associated with impaired endocannabinoid signaling in mice with a deletion of the glutamate transporter GLAST. *Neuropharmacology* 2012;63:181–9.
22. Karlsson RM, Tanaka K, Saksida LM, Bussey TJ, Heilig M, Holmes A. Assessment of glutamate transporter GLAST (EAAT1)-deficient mice for phenotypes relevant to the negative and executive/cognitive symptoms of schizophrenia. *Neuropsychopharmacology* 2009;34:1578–89.
23. Aroeira RI, Sebastiao AM, Valente CA. GlyT1 and GlyT2 in brain astrocytes: expression, distribution and function. *Brain Struct Funct.* 2014;219:817–30.
24. Newman EA. New roles for astrocytes: regulation of synaptic transmission. *Trends Neurosci.* 2003;26:536–42.
25. Do KQ, Benz B, Sorg O, Pellerin L, Magistretti PJ. beta-Adrenergic stimulation promotes homocysteic acid release from astrocyte cultures: evidence for a role of astrocytes in the modulation of synaptic transmission. *J Neurochemistry.* 1997;68:2386–94.
26. Chan CY, Sun HS, Shah SM, Agovic MS, Friedman E, Banerjee SP. Modes of direct modulation by taurine of the glutamate NMDA receptor in rat cortex. *Eur J Pharmacol.* 2014;728:167–75.
27. Corkrum M, Covelo A, Lines J, Bellocchio L, Pisansky M, Loke K, et al. Dopamine-evoked synaptic regulation in the nucleus accumbens requires astrocyte activity. *Neuron* 2020;105:1036–47. e5
28. Mehler-Wex C, Riederer P, Gerlach M. Dopaminergic dysbalance in distinct basal ganglia neurocircuits: implications for the pathophysiology of Parkinson's disease, schizophrenia and attention deficit hyperactivity disorder. *Neurotox Res.* 2006;10:167–79.
29. Del Casale A, Kotzalidis GD, Rapinesi C, Serata D, Ambrosi E, Simonetti A, et al. Functional neuroimaging in obsessive-compulsive disorder. *Neuropsychobiology* 2011;64:61–85.
30. Hemmerle AM, Herman JP, Seroogy KB. Stress, depression and Parkinson's disease. *Exp Neurol.* 2012;233:79–86.
31. Graybiel AM, Grafton ST. The striatum: where skills and habits meet. *Cold Spring Harb Perspect Biol.* 2015;7:a021691.
32. Kupferschmidt DA, Juczewski K, Cui G, Johnson KA, Lovinger DM. Parallel, but dissociable, processing in discrete corticostriatal inputs encodes skill learning. *Neuron* 2017;96:476–89. e5
33. Yin HH, Mulcare SP, Hilario MR, Clouse E, Holloway T, Davis MI, et al. Dynamic reorganization of striatal circuits during the acquisition and consolidation of a skill. *Nat Neurosci.* 2009;12:333–41.
34. Lipton DM, Gonzales BJ, Citri A. Dorsal striatal circuits for habits, compulsions and addictions. *Front Syst Neurosci.* 2019;13:28.
35. Domi E, Domi A, Adermark L, Heilig M, Augier E. Neurobiology of alcohol seeking behavior. *J Neurochem.* 2021;157:1585–614.
36. Lovinger DM, Gremel CM. A circuit-based information approach to substance abuse research. *Trends Neurosci.* 2021;44:122–35.
37. Adermark L, Lovinger DM. Electrophysiological properties and gap junction coupling of striatal astrocytes. *Neurochem Int.* 2008;52:1365–72.
38. Adermark L, Lovinger DM. Ethanol effects on electrophysiological properties of astrocytes in striatal brain slices. *Neuropharmacology* 2006;51:1099–108.
39. Cavaccini A, Durkee C, Kofuji P, Tonini R, Araque A. Astrocyte signaling gates long-term depression at corticostriatal synapses of the direct pathway. *J Neurosci: Off J Soc Neurosci.* 2020;40:5757–68.
40. Fonnum F, Johnsen A, Hassel B. Use of fluorocitrate and fluoroacetate in the study of brain metabolism. *Glia* 1997;21:106–13.
41. Hassel B, Paulsen RE, Johnsen A, Fonnum F. Selective inhibition of glial cell metabolism in vivo by fluorocitrate. *Brain Res.* 1992;576:120–4.
42. Hassel B, Bachelard H, Jones P, Fonnum F, Sonnewald U. Trafficking of amino acids between neurons and glia in vivo. Effects of inhibition of glial metabolism by fluoroacetate. *J Cereb Blood Flow Metab.* 1997;17:1230–8.
43. Willoughby JO, Mackenzie L, Broberg M, Thoren AE, Medvedev A, Sims NR, et al. Fluorocitrate-mediated astroglial dysfunction causes seizures. *J Neurosci Res.* 2003;74:160–6.
44. Lian XY, Stringer JL. Energy failure in astrocytes increases the vulnerability of neurons to spreading depression. *Eur J Neurosci.* 2004;19:2446–54.
45. Largo C, Cuevas P, Somjen GG, Martin del Rio R, Herreras O. The effect of depressing glial function in rat brain in situ on ion homeostasis, synaptic transmission, and neuron survival. *J Neurosci.* 1996;16:1219–29.
46. Padmashri R, Suresh A, Boska MD, Dunaevsky A. Motor-skill learning is dependent on astrocytic activity. *Neural Plast.* 2015;2015:938023.
47. Licheri V, Eckernas D, Bergquist F, Ericson M, Adermark L. Nicotine-induced neuroplasticity in striatum is subregion-specific and reversed by motor training on the rotarod. *Addict Biol.* 2020;25:e12757.
48. Zielke HR, Zielke CL, Baab PJ. Direct measurement of oxidative metabolism in the living brain by microdialysis: a review. *J Neurochem.* 2009;109:24–9. Suppl 1
49. Hassel B, Westergaard N, Schousboe A, Fonnum F. Metabolic differences between primary cultures of astrocytes and neurons from cerebellum and cerebral cortex. Effects of fluorocitrate. *Neurochem Res.* 1995;20:413–20.
50. Zielke HR, Zielke CL, Baab PJ, Tildon JT. Effect of fluorocitrate on cerebral oxidation of lactate and glucose in freely moving rats. *J Neurochem.* 2007;101:9–16.
51. Clarke RB, Soderpalm B, Lotfi A, Ericson M, Adermark L. Involvement of inhibitory receptors in modulating dopamine signaling and synaptic activity following acute ethanol exposure in striatal subregions. *Alcohol Clin Exp Res.* 2015;39:2364–74.
52. Ulenius L, Andren A, Adermark L, Soderpalm B, Ericson M. Sub-chronic taurine administration induces behavioral sensitization but does not influence ethanol-induced dopamine release in the nucleus accumbens. *Pharm Biochem Behav.* 2020;188:172831.
53. Licheri V, Lagstrom O, Lotfi A, Patton MH, Wigstrom H, Mathur B, et al. Complex control of striatal neurotransmission by nicotinic acetylcholine receptors via excitatory inputs onto medium spiny neurons. *J Neurosci.* 2018;38:6597–607.
54. Adermark L, Clarke RB, Soderpalm B, Ericson M. Ethanol-induced modulation of synaptic output from the dorsolateral striatum in rat is regulated by cholinergic interneurons. *Neurochem Int.* 2011;58:693–9.
55. Chai H, Diaz-Castro B, Shigetomi E, Monte E, Oceau JC, Yu X, et al. Neural circuit-specialized astrocytes: transcriptomic, proteomic, morphological, and functional evidence. *Neuron* 2017;95:531–49. e9
56. Nagai J, Rajbhandari AK, Gangwani MR, Hachisuka A, Coppola G, Masmanidis SC, et al. Hyperactivity with disrupted attention by activation of an astrocyte synaptogenic cue. *Cell* 2019;177:1280–92. e20

57. Atwood BK, Kupferschmidt DA, Lovinger DM. Opioids induce dissociable forms of long-term depression of excitatory inputs to the dorsal striatum. *Nat Neurosci*. 2014;17:540–8.
58. Adermark L, Lovinger DM. Combined activation of L-type Ca<sup>2+</sup> channels and synaptic transmission is sufficient to induce striatal long-term depression. *J Neurosci*. 2007;27:6781–7.
59. Paulsen RE, Fonnun F. Role of glial cells for the basal and Ca<sup>2+</sup>-dependent K<sup>+</sup>-evoked release of transmitter amino acids investigated by microdialysis. *J Neurochem*. 1989;52:1823–9.
60. Hennes M, Lombaert N, Wahis J, Van den Haute C, Holt MG, Arckens L. Astrocytes shape the plastic response of adult cortical neurons to vision loss. *Glia* 2020;68:2102–18.
61. Li Puma DD, Marocci ME, Lazzarino G, De Chiara G, Tavazzi B, Palamara AT, et al. Ca<sup>2+</sup>-dependent release of ATP from astrocytes affects herpes simplex virus type 1 infection of neurons. *Glia* 2021;69:201–15.
62. Zafra F, Ibanez I, Bartolome-Martin D, Piniella D, Arribas-Blazquez M, Gimenez C. Glycine transporters and its coupling with NMDA receptors. *Adv Neurobiol*. 2017;16:55–83.
63. Shibasaki K, Hosoi N, Kaneko R, Tominaga M, Yamada K. Glycine release from astrocytes via functional reversal of GlyT1. *J Neurochemistry*. 2017;140:395–403.
64. Ishiwata S, Umino A, Nishikawa T. Involvement of neuronal and glial activities in control of the extracellular d-serine concentrations by the AMPA glutamate receptor in the mouse medial prefrontal cortex. *Neurochemistry Int*. 2018;119:120–25.
65. Dopic JO, Gonzalez-Hernandez T, Perez IM, Garcia IG, Abril AM, Inchausti JO, et al. Glycine release in the substantia nigra: Interaction with glutamate and GABA. *Neuropharmacology* 2006;50:548–57.
66. Trabelsi Y, Amri M, Becq H, Molinari F, Aniksztejn L. The conversion of glutamate by glutamine synthase in neocortical astrocytes from juvenile rat is important to limit glutamate spillover and peri/extrasynaptic activation of NMDA receptors. *Glia* 2017;65:401–15.
67. Reiner A, Levitz J. Glutamatergic signaling in the central nervous system: ionotropic and metabotropic receptors in concert. *Neuron* 2018;98:1080–98.
68. Schousboe A. Metabolic signaling in the brain and the role of astrocytes in control of glutamate and GABA neurotransmission. *Neurosci Lett*. 2019;689:11–13.
69. Hertz L, Rothman DL. Glutamine-glutamate cycle flux is similar in cultured astrocytes and brain and both glutamate production and oxidation are mainly catalyzed by aspartate aminotransferase. *Biology (Basel)*. 2017;6:17.
70. Untiet V, Kovermann P, Gerkau NJ, Gensch T, Rose CR, Fahlke C. Glutamate transporter-associated anion channels adjust intracellular chloride concentrations during glial maturation. *Glia* 2017;65:388–400.
71. Mishra D, Harrison NR, Gonzales CB, Schilström B, Konradsson-Geuken A. Effects of age and acute ethanol on glutamatergic neurotransmission in the medial prefrontal cortex of freely moving rats using enzyme-based microelectrode amperometry. *PLoS one*. 2015;10:e0125567.
72. Asanuma M, Miyazaki I, Murakami S, Diaz-Corrales FJ, Ogawa N. Striatal astrocytes act as a reservoir for L-DOPA. *PLoS one*. 2014;9:e106362.
73. Adermark L, Clarke RB, Olsson T, Hansson E, Soderpalm B, Ericson M. Implications for glycine receptors and astrocytes in ethanol-induced elevation of dopamine levels in the nucleus accumbens. *Addict Biol*. 2011;16:43–54.
74. Roberts BM, Doig NM, Brimblecombe KR, Lopes EF, Siddorn RE, Threlfell S, et al. GABA uptake transporters support dopamine release in dorsal striatum with maladaptive downregulation in a parkinsonism model. *Nat Commun*. 2020;11:4958.
75. Ericson M, Molander A, Stomberg R, Soderpalm B. Taurine elevates dopamine levels in the rat nucleus accumbens; antagonism by strychnine. *Eur J Neurosci*. 2006;23:3225–9.
76. Wu HQ, Rassoulpour A, Schwarcz R. Kynurenic acid leads, dopamine follows: a new case of volume transmission in the brain? *J Neural Transm (Vienna)*. 2007;114:33–41.
77. Solis O, Garcia-Sanz P, Herranz AS, Asensio MJ, Moratalla RL-DOPA. Reverses the increased free amino acids tissue levels induced by dopamine depletion and rises GABA and tyrosine in the striatum. *Neurotox Res*. 2016;30:67–75.
78. Morales I, Fuentes A, Ballaz S, Obeso JA, Rodriguez M. Striatal interaction among dopamine, glutamate and ascorbate. *Neuropharmacology* 2012;63:1308–14.
79. Agren R, Sahlholm K. Voltage-dependent dopamine potency at D1-like dopamine receptors. *Front Pharmacol*. 2020;11:581151.
80. Fasano C, Bourque MJ, Lapointe G, Leo D, Thibault D, Haber M, et al. Dopamine facilitates dendritic spine formation by cultured striatal medium spiny neurons through both D1 and D2 dopamine receptors. *Neuropharmacology* 2013;67:432–43.
81. Adermark L, Lovinger DM. Frequency-dependent inversion of net striatal output by endocannabinoid-dependent plasticity at different synaptic inputs. *J Neurosci*. 2009;29:1375–80.
82. Calabresi P, Maj R, Pisani A, Mercuri NB, Bernardi G. Long-term synaptic depression in the striatum: physiological and pharmacological characterization. *J Neurosci: Off J Soc Neurosci*. 1992;12:4224–33.
83. Shen W, Chen S, Liu Y, Han P, Ma T, Zeng LH. Chemogenetic manipulation of astrocytic activity: is it possible to reveal the roles of astrocytes? *Biochemical Pharmacol*. 2021;186:114457.
84. Durkee CA, Covelo A, Lines J, Kofuji P, Aguilar J, Araque A. Gi/o protein-coupled receptors inhibit neurons but activate astrocytes and stimulate gliotransmission. *Glia* 2019;67:1076–93.
85. Kang S, Hong SI, Lee J, Peyton L, Baker M, Choi S, et al. Activation of astrocytes in the dorsomedial striatum facilitates transition from habitual to goal-directed reward-seeking behavior. *Biol Psychiatry*. 2020;88:797–808.

## ACKNOWLEDGEMENTS

We acknowledge the assistance provided by Karin Ademar during immunohistochemical stainings, and Erika Lucente and Davide Cadeddu during whole cell recordings. We also acknowledge the Viral Vector Facility (VVF) of the Neuroscience Center Zurich for producing the viral vectors and viral vector plasmids used in this study, as well as the Center for Cellular Imaging at the Sahlgrenska Academy, University of Gothenburg, and the National Microscopy Infrastructure, NMI (VR-RFI 2016-00968) for providing assistance in microscopy and for the opportunity to use their imaging equipment and cryostat.

## AUTHOR CONTRIBUTIONS

L.A. designed the study, conducted electrophysiological recordings, assembled figures, and drafted the manuscript. O.L. performed immunohistochemistry and electrophysiological recordings. A.L. performed microdialysis. V.L. performed whole cell recordings. A.H., E.A.L., and A.D. conducted electrophysiological field potential recordings. R.S. performed viral injections and assisted during microdialysis. B.S. and M.E. assisted in data interpretation. All authors critically revised the manuscript for important intellectual content and contributed to the final draft of the manuscript.

## FUNDING

This work was supported by the Swedish research council (vetenskapsrådet: Dnr: 2018-02814, 2020-00559, 2020-01346, and 2020-02105), Stiftelsen Psykiatriska Forskningsfonden, Arvid Carlssons stiftelse, Kungliga Vetenskaps- och Vitterhets-Samhället i Göteborg, Thuring's stiftelse, Wilhelm och Martina Lundgrens vetenskapsfond, Magnus Bergvall's Foundation.

## COMPETING INTERESTS

The authors declare no competing interests.

## ADDITIONAL INFORMATION

**Correspondence** and requests for materials should be addressed to Louise Adermark.

**Reprints and permission information** is available at <http://www.nature.com/reprints>

**Publisher's note** Springer Nature remains neutral with regard to jurisdictional claims in published maps and institutional affiliations.